

Assessing cotton defoliation, regrowth control and root rot infection using remote sensing technology

Chenghai Yang¹, Shoil M. Greenberg¹, James H. Everitt¹, Carlos J. Fernandez²

(1. USDA-ARS, Kika de la Garza Subtropical Agricultural Research Center, Weslaco, Texas 78596, USA;

2. Texas AgriLife Research and Extension Center, Corpus Christi, Texas 78406, USA)

Abstract: Cotton defoliation and post-harvest destruction are important cultural practices for cotton production. Cotton root rot is a serious and destructive disease that affects cotton yield and lint quality. This paper presents an overview and summary of the methodologies and results on the use of remote sensing technology for evaluating cotton defoliation and regrowth control methods and for assessing cotton root rot infection based on published studies. Ground reflectance spectra and airborne multispectral and hyperspectral imagery were used in these studies. Ground reflectance spectra effectively separated different levels of defoliation and airborne multispectral imagery permitted both visual and quantitative differentiations among defoliation treatments. Both ground reflectance and airborne imagery were able to differentiate cotton regrowth among different herbicide treatments for cotton stalk destruction. Airborne multispectral and hyperspectral imagery accurately identified root rot-infected areas within cotton fields. Results from these studies indicate that remote sensing can be a useful tool for evaluating the effectiveness of cotton defoliation and regrowth control strategies and for detecting and mapping root rot damage in cotton fields. Compared with traditional visual observations and ground measurements, remote sensing techniques have the potential for effective and accurate assessments of various cotton production operations and pest conditions.

Keywords: remote sensing, cotton defoliation, regrowth control, root rot, reflectance spectrum, airborne multispectral imagery, airborne hyperspectral imagery

DOI: 10.3965/j.issn.1934-6344.2011.04.001-011

Citation: Yang C, Greenberg S M, Everitt J H, Fernandez C J. Assessing cotton defoliation, regrowth control and root rot infection using remote sensing technology. Int J Agric & Biol Eng, 2011; 4(4): 1–11.

1 Introduction

Use of defoliant to prepare the cotton crop for machine harvest has been an accepted practice for expediting crop maturity, increasing harvest efficiency, and improving lint yield and quality. Picker cotton is usually treated with a hormonal or herbicidal defoliant to remove the leaves, while stripper cotton is treated with a defoliant followed by a desiccant or simply with a once-over desiccant in low-yielding fields^[1,2]. Field evaluations of defoliant are very important for

identifying the optimal rate for a single defoliant or a combination of two or more defoliant for effective defoliation. Traditional approaches for these evaluations are based on visual observations and ground measurements^[3].

Cotton stalk destruction following harvest is an important cultural practice for managing overwintering boll weevils (*Anthonomus grandis grandis* Boheman) and other insects such as the silverleaf whitefly (*Bemisia argentifolii* Bellows and Perring) and the pink bollworm *Pectinophora gossypiella* (Saunders)]^[4]. The boll weevil eradication programs recently implemented in the Rio Grande Valley and other Texas counties may help eliminate the insect pest in the future, but cotton stalk destruction remains an important part of the eradication programs and is still enforced by Texas law.

Received date: 2011-11-12 **Accepted date:** 2011-12-11

Corresponding author: Chenghai Yang, PhD, Agricultural Engineer, USDA-ARS, Weslaco, Texas, 78596. Phone: 956-969-4837; Fax: 956-969-4893; Email: chenghai.yang@ars.usda.gov.

Mechanical destruction methods such as shredding followed by plowing are generally effective, but recent increases in minimum tillage and no tillage systems make herbicide applications an attractive alternative. Sparks et al.^[5] evaluated the efficacy of Savage (2,4-D) and Harmony Extra for post-harvest cotton stalk destruction. Norman et al.^[4] conducted greenhouse and field experiments to evaluate 2,4-D and other herbicides under different application timings for cotton regrowth control. In both studies, they used visual ratings and plant physical measurements to quantify the differences among several stalk destruction treatments.

Traditional approaches for cotton defoliation and regrowth control seem to be simple and workable, but tend to be time-consuming if a large number of treatments over an extensive area are involved. From the perspective of remote sensing, cotton plants treated with different defoliant would have different spectral responses from normally growing plants. Similarly, regrowth from shredded cotton stalks treated with different herbicides would have different spectral responses from non-treated regrowth. Yang et al.^[6] evaluated the effectiveness of different cotton defoliation treatments using field reflectance spectra and airborne multispectral imagery. Yang et al.^[7,8] examined the feasibility of ground reflectance measurements and airborne multispectral imagery for evaluating the effectiveness of various different herbicide treatments for cotton regrowth control as compared with traditional visual observations and ground measurements.

Cotton root rot, also known as *Phymatotrichum* root rot or Texas root rot, is caused by the soil-borne fungus *Phymatotrichum omnivorum*^[9]. The fungus spreads from plant to plant either through root contact or by slow growth of mycelial strands through the soil. Once infected, the plant first turns yellow or brown and then wilts rapidly. The disease significantly reduces cotton yield and lowers lint quality^[10,11]. Cotton root rot is a difficult plant disease to control. Several cultural practices have been recommended to reduce the occurrence and severity of the disease, but they are not always effective. Fungicides and fumigants can reduce the occurrence and severity of the disease, but they are

not always effective due to the ability of the fungus to survive deep in the soil^[12-14]. Since most fungicides and fumigants can only penetrate a limited distance into the soil, chemical treatments have to be applied every year or every few years in order to suppress the disease. This approach can become prohibitively expensive if the whole field is to be treated. An effective strategy would be to define the infected areas within the field for site-specific chemical application to manage the disease.

Remote sensing provides a convenient and useful means of recording the extent of root rot damage by detecting changes in the plant canopy. Taubenhaus et al.^[15] photographed cotton fields infected by the root rot fungus from an airplane. Nixon et al.^[16] used aerial color-infrared (CIR) photography to document the distributions of cotton root rot damage and detect the change in root rot areas after chemical treatments. Nixon et al.^[17] evaluated multispectral video imagery for the detection of cotton root rot. With recent advances in remote sensing, global positioning systems (GPS), and image processing techniques, this disease can be more effectively detected and mapped for management. Yang et al.^[18] evaluated airborne multispectral imagery for detecting and mapping root rot damage in cotton fields for the management of the disease. Yang et al.^[19] compared airborne multispectral and hyperspectral imagery for detecting and mapping root rot damage in cotton fields.

This paper provides an overview and summary of the methodologies and results on the use of remote sensing techniques for evaluating cotton defoliation and regrowth control and for mapping cotton root rot infection on the basis of five published studies^[6-8,18,19]. Although each of the studies was conducted on multiple fields, results from one field for each study will be used to illustrate the applications.

2 Materials and Methods

2.1 Study sites and experimental designs

2.1.1 Cotton defoliation

A field experiment was conducted on an irrigated cotton field located at the South Research Farm of the USDA-ARS Kika de la Garza Subtropical Agricultural

Research Center in Weslaco, Texas, in 2001. Shortly before cotton defoliation, eight treatments, including one control and seven combinations of defoliant and insecticides (Table 1), with three replications were assigned across 24 experimental plots in a randomized complete block design within the field^[6]. For comparison with remote sensing results, leaf counts were taken from ten randomly selected plants within each plot for the field six days after the application. Percent defoliation was calculated from the mean number of leaves per plant within each plot and the mean number of leaves per plant in the control.

Table 1 Defoliant and insecticide treatments for a cotton field

Treatment ^[a]	Defoliant	Insecticide
1. Control	--	--
2. Def + Dropp + Guthion	Def (half rate) + Dropp (half rate)	Guthion (half rate)
3. Def + Dropp	Def (half rate) + Dropp (half rate)	--
4. Dropp + Guthion	Dropp (full rate)	Guthion (full rate)
5. Def + Guthion	Def (full rate)	Guthion (half rate)
6. Def + Karate	Def (full rate)	Karate (half rate)
7. Guthion	--	Guthion (full rate)
8. Karate	--	Karate (full rate)

Note: ^[a] Full rate of Def = 2 pt/ac or 2.34 L/ha; full rate of Dropp = 0.2 lb/ac or 224 g/ha; full rate of Guthion = 0.25 lb AI/ac or 280 g AI/ha; and full rate of Karate = 0.033 lb AI/ac or 37 g AI/ha.

2.1.2 Cotton regrowth control

A field experiment was conducted in 2002 on an irrigated cotton field located at "Hiler" Annex Farm of the Texas Agricultural Research and Extension Center in Weslaco, Texas. Eight treatments (combinations of two herbicides and four application timings) were assigned to four blocks in a randomized complete block design^[8]. For comparison with remote sensing results, plant regrowth in each plot was visually rated on a 1-to-5 scale based on the ratings used by Sparks et al.^[5]. The ratings were as follows: 1 = no live plants; 2 = some plants alive, but appear sick; 3 = most plants alive, but appear sick; 4 = some plants appear healthy; and 5 = most plants appear healthy.

2.1.3 Cotton root rot

One center-pivot irrigated cotton field (105 ha) near Corpus Christi, Texas was selected for evaluating multispectral imagery for mapping root rot in 2001^[18].

Another center-pivot irrigated cotton field (55 ha) in the nearby area was selected for comparing multispectral and hyperspectral imagery for mapping this disease in 2002^[19]. These fields had a history of cotton root rot. Standard production practices common in the region were used in the fields. No particular treatment was applied to the fields to control root rot.

2.2 Remote sensing data collection

2.2.1 Reflectance spectra

A FieldSpec HandHeld spectroradiometer (Analytical Spectral Devices, Inc., Boulder, Colorado) was used for reflectance data collection. The instrument was sensitive in the 350 to 1 050 nm portion of the spectrum with a nominal spectral resolution of 1.4 nm. Reflectance spectra were taken on randomly selected canopies from each plot and each spectrum was an average of 10 sample spectra over each canopy. The instrument had a field of view angle of 25° and was held at 1 m above the canopy during data collection, resulting in a circular target area of 44 cm in diameter. Reflectance measurements were made between 1 130 h and 1 430 h local time under sunny conditions.

2.2.2 Airborne multispectral and hyperspectral imagery

Airborne CIR imagery was acquired using a digital imaging system described by Escobar et al.^[20]. The imaging system consisted of three charge-coupled device (CCD) cameras and a computer equipped with three image-digitizing boards that had the capability of obtaining 8-bit images with 1 024×1 024 pixels. The three cameras were filtered for spectral observations in the green (555-565 nm), red (625-635 nm), and NIR (845-857 nm) wavelength intervals, respectively. The original imaging system was upgraded in 2002 to obtain images with 1 280×1 024 pixels in the same spectral wavebands. Thus, the imagery for the defoliation study and the root rot study conducted in 2001 had 1 024×1 024 pixels, while imagery for the regrowth control study and root rot study conducted in 2002 had 1 280×1 024 pixels.

Airborne hyperspectral imagery was acquired using an airborne imaging system described by Yang et al.^[21]. The system was configured to acquire 128-band imagery with 640-pixel swath and 12-bit pixel depth in the 457-922 nm spectral range. A Cessna 206 aircraft was

used to acquire imagery between 1 130 h and 1 430 h local time under sunny conditions. The ground pixel size achieved for the multispectral imagery was 0.2 m for the defoliation study in 2001, 0.3 m for the regrowth control study in 2002, and 1.3 m for the root rot study in 2001. The ground pixel size achieved was 1.2 m for the multispectral imagery and 2.4 m for the hyperspectral imagery in 2002. For radiometric calibration of the imagery, four 8 m × 8 m tarpaulins with nominal reflectance values of 4%, 16%, 32% and 48%, respectively, were placed near the study sites during image acquisition for the regrowth control study. The actual reflectance values from the tarpaulins were measured using the spectroradiometer.

2.3 Image processing and data analysis

The NIR and green band images in each CIR composite were registered to the red band image to correct the misalignments among the three bands. The registered images were then georeferenced or rectified to the Universal Transverse Mercator (UTM), World Geodetic Survey 1984 (WGS-84), Zone 14, coordinate system based on ground control points around each field located with a submeter-accuracy Trimble GPS Pathfinder Pro XRS receiver (Trimble Navigation Limited, Sunnyvale, California). The hyperspectral imagery was rectified to the respective multispectral imagery in 2002. The rectified images for the regrowth study were converted to reflectance based on three calibration equations (one for each band) relating reflectance values to the digital count values extracted from the tarpaulins on the imagery.

To extract reflectance values for each of the experimental plots in the defoliation study, rectangular areas defining the plots were overlaid on the imagery. Pixel values within a plot were extracted from each band image and averaged as the reflectance value for the band. For the regrowth control study, the reflectance values were extracted from individual rows within each plot. Four vegetation indices were calculated from the reflectance values for the three bands to measure vegetation vigor and abundance^[22]. Two of the vegetation indices were band ratios defined as $NR = NIR/Red$ and $NG = NIR/Green$. The other two were the

$NDVI$ and the green $NDVI$ ($GNDVI$) defined as $NDVI = (NIR-Red)/(NIR+Red)$ and $GNDVI = (NIR-Green)/(NIR+Green)$. Analysis of variance was performed on the vegetation indices as well as on percent defoliation for the defoliation study and visual rating for the regrowth control study. Multiple comparisons on means were made using Fisher's protected least significant difference (LSD) procedure (SAS Institute Inc., Cary, North Carolina).

The rectified images for the cotton root rot studies were classified into healthy and root rot areas using unsupervised classification^[23]. For accuracy assessment of the classification maps, 50 points were assigned to the two categories in a stratified random pattern within each field. The geographic coordinates of these points were determined, and the Trimble GPS system was used to navigate to these points for ground verification. The plants and their roots were visually examined for cotton root rot symptoms, and the actual categories of the points were determined based on whether the plants at and surrounding the points were infected by the fungus.

To compare cotton yield and fiber quality between the root rot zones and healthy zones, plant physical measurements were made at 20 of the 50 points used for accuracy assessment, with 10 points from root rot zones and 10 from the healthy zones. Cotton fiber quality was analyzed with a High-Volume Instrument (HVI) testing system by the Fiber Quality Lab of Cotton Incorporated in Cary, North Carolina. The quantified fiber properties include micronaire (MIC), upper half mean length (UHM), length uniformity index (UI), strength, and color as the degree of reflectance (Rd) and yellowness (+b)^[24]. Yield and fiber quality data were analyzed by the analysis of variance procedure, and means were separated using Fisher's LSD procedure.

3 Results and discussion

3.1 Cotton defoliation

Figure 1 presents the reflectance spectra of cotton plants obtained from the defoliated cotton field six days after chemical application. For comparison, the spectrum for bare soil in the field is also shown. Since spectra from some of the eight treatments are similar and

difficult to differentiate, only the spectra from treatments 1, 2, and 6 are presented. As shown in table 1, treatment 1 was the control, treatment 2 received two defoliants (Def and Dropp) and one insecticide (Guthion) all at half rate, and treatment 6 received Def at full rate and another insecticide (Karate) at half rate. The spectra for treatments 2 and 6 were different from that of the control. The reflectance of the defoliated plants was higher in the visible portion and lower in the NIR portion of the spectrum than the reflectance of healthy plants. Since defoliated plants had fewer leaves than healthy plants, the reflectance taken from the defoliated plants represented a combination of reflectance values from both the plants and the bare soil. Therefore, the spectra for defoliated plants fell between the spectra for healthy plants and bare soil. The higher the defoliation, the closer the spectrum should be to that of bare soil. However, even completely defoliated plants will not have the same reflectance curve as bare soil because soil exposure is reduced as leaves fall from the plants. Based on the spectra of different treatments relative to the spectra of healthy plants and bare soil, the effectiveness of defoliation can be evaluated. For example, treatment 2 had better defoliation than treatment 6 in this particular experiment because the spectrum for treatment 2 was closer to that of bare soil.

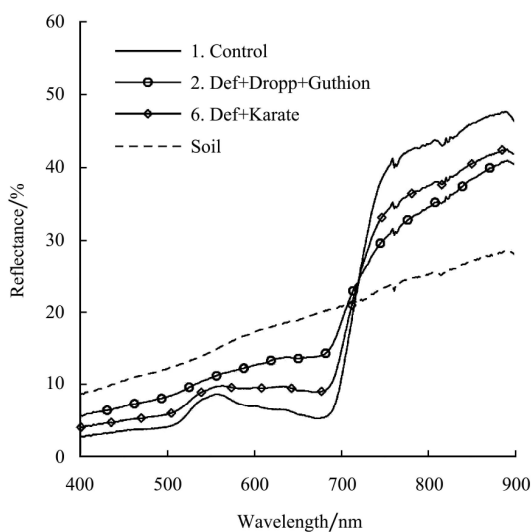


Figure 1 Reflectance spectra of cotton plants obtained six days after chemical application for three of the eight treatments. For comparison, the spectrum for bare soil in the field is also shown

from the defoliated cotton field six days after chemical application. Differences among the treatments can be clearly seen from the CIR image. On the CIR image, healthy plants showed a reddish-magenta tone, while defoliated plants had a light gray or pinkish color.

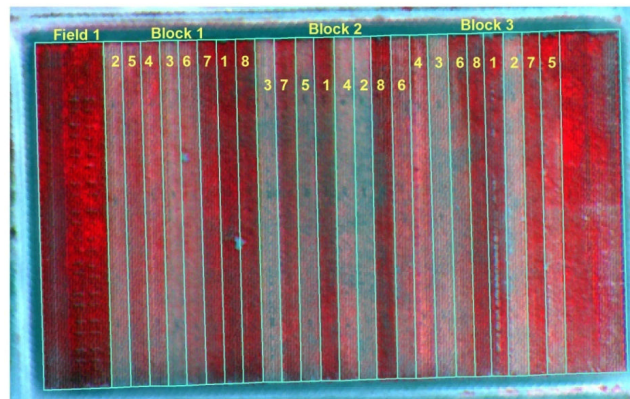


Figure 2 A color-infrared image acquired from a cotton field six days after different defoliation treatments were applied

Table 2 shows the mean NDVI values based on the CIR image and the mean percent defoliation relative to the control based on ground observations six days after defoliation treatments. Since plants with fewer leaves have lower NDVI values than plants with more leaves, better defoliation corresponded to lower NDVI values. The data in Table 2 clearly indicate three distinct groups among the eight treatments. Treatments 1, 7, and 8, which had the highest NDVI values, had the least defoliation. In fact, these three treatments did not receive any defoliants, although treatments 7 and 8 received two insecticides, Guthion and Karate at half rates, respectively. No defoliation effect from the two insecticides was detected. Treatments 2 and 3 had the lowest NDVI values, representing the best defoliation treatments. Both treatments 2 and 3 received Def and Dropp at half rates, though treatment 3 also received Guthion at half rate. Again, Guthion did not have a detectable effect on defoliation. Treatments 4, 5, and 6, which received varying levels of defoliants and insecticides, were not as effective as treatments 2 and 3, but still caused significant defoliation.

The ground observation results shown in Table 2 agree well with those from the airborne imagery. The airborne image considered every pixel across the entire field, while the ground observations relied on only ten

Figure 2 shows the CIR composite image acquired

plants per plot. Therefore, the remote sensing-based approach should offer more efficient and accurate evaluation of various defoliation strategies than commonly used ground observation and measurement approaches.

Table 2 Mean NDVI values based on a CIR image and mean percent defoliation relative to the control based on ground observations six days after defoliation treatments for a cotton field

Treatment	NDVI	Percent defoliation
1. Control	0.310a ^[a]	0.0a
2. Def + Dropp + Guthion	0.085c	93.6c
3. Def + Dropp	0.086c	90.7c
4. Dropp + Guthion	0.177b	66.8b
5. Def + Guthion	0.204b	59.8b
6. Def + Karate	0.188b	72.3b
7. Guthion	0.318a	1.3a
8. Karate	0.316a	4.4a

Note: ^[a] Means within a column followed by the same letter are not significantly different at the 0.05 level.

3.2 Cotton regrowth control

Figure 3 presents the reflectance spectra of cotton regrowth for three of the eight herbicide treatments in the 2002 experiment. The spectra for normal regrowth (without herbicide treatment) and bare soil are also shown in the graph for comparison. The spectrum for normal regrowth had the shape of a typical spectral curve for healthy plants^[25] and the spectrum for bare soil was essentially a straight line. If regrowth for a treatment is lush and abundant, the spectrum for the regrowth will be close to that for normal regrowth; otherwise, the spectrum will be close to that of the soil. This spectral behavior is the basis for the separation of different levels of cotton regrowth. The spectra for the three treatments were closer to the soil spectrum than to the spectrum of normal growth (Figure 3), indicating that these herbicide treatments significantly limited cotton regrowth. Based on field observations, normal regrowth in the untreated reference area was very healthy and had a width of approximately 50 cm at the time of reflectance data collection, while regrowth in all the plots treated with herbicides exhibited obvious injury and had a width ranging from zero (no regrowth) to about 25 cm.

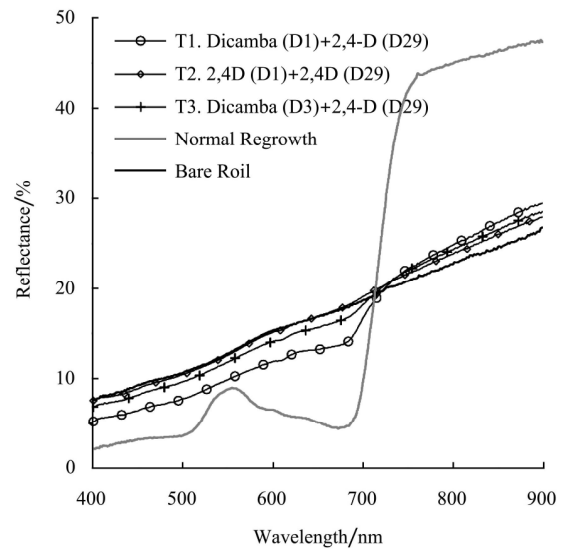


Figure 3 Reflectance spectra of cotton regrowth, measured 36 days after stalk shredding, for three of the eight herbicide treatments for a 2002 experiment. D1 and D3 represent applying the herbicides initially 14 hours and 3 days, respectively, after cotton stalks were shredded. A second application of 2,4-D was made to all treatments 29 days (D29) after cotton stalks were shredded. The rates were 1.06 kg ai/ha of 2,4-D and 0.82 kg ai/ha of dicamba for each application

As mentioned previously, the spectroradiometer covered a circular area with a diameter of 44 cm, which was much larger than the width of the regrowth in the treatment plots. Moreover, the regrowth had unhealthy and sparse leaves. Therefore, the spectra for all the treatments were mainly the spectral response from the soil background. Nevertheless, regrowth in all treatments caused the spectra to deviate slightly from the soil spectrum. Based on the levels of deviation, treatment 2, which had an initial application of 2,4-D 14 hours after shredding and a second application of 2,4-D 29 days after shredding, appeared to be more effective than the other two treatments. Treatment 1, which had an initial application of dicamba 14 hours after shredding and a second application of 2,4-D 29 days after shredding, didn't perform as well as treatment 3 for which Dicamba was initially applied three days after shredding.

Ground reflectance spectra can be a useful tool for differentiating the effectiveness of various herbicide treatments. However, spectral measurements can be easily affected by spatial variability within treatments, limited amounts of regrowth, and variations in the field of

view of the spectroradiometer. To minimize the effects of these factors, a large number of spectral samples are needed to obtain accurate and reliable spectra.

Figure 4 shows a CIR image acquired from the experimental plots on 27 August 2002, 36 days after cotton stalks were shredded. Eight rows of cotton plants at the bottom of the image (the south side of the field) were not shredded after harvest and new leaves regrew on the original stalks. Plants in the untreated reference area were regrowth from shredded stalks without any herbicide treatment, though some of the rows in the area were sprayed during equipment adjustment. Regrowth from the eight non-shredded rows and the untreated area was healthy and vegetative and appeared bright red on the CIR image. The buffers separating the plots were not as vegetative because of the drift from herbicide applications, but had a reddish tone and could be easily identified on the image. Regrowth in the treatment plots was generally small and had a brownish and grayish color. Nevertheless, regrowth for treatments 1 and 7 could be distinguished from the other treatments on the image. Regrowth in these plots was large enough to show a reddish tone along the rows in the image, while regrowth for the other six treatments was so small and unhealthy that it was extremely difficult to visually differentiate among them.

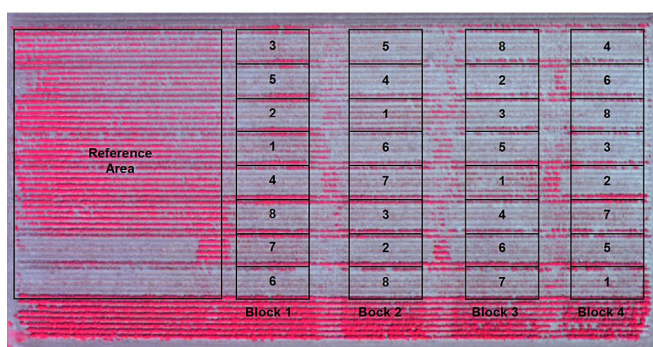


Figure 4 Color-infrared digital image of a cotton field acquired 36 days after cotton stalks were shredded. The eight treatments are defined as follows: 1. Dicamba (D1) + 2,4-D (D29); 2. 2,4-D (D1) + 2,4-D (D29); 3. Dicamba (D3) + 2,4-D (D29); 4. 2,4-D (D3) + 2,4-D (D29); 5. Dicamba (D7) + 2,4-D (D29); 6. 2,4-D (D7) + 2,4-D (D29); 7. Dicamba (D14) + 2,4-D (D29); and 8. 2,4-D (D14) + 2,4-D (D29). Application rates were 1.06 kg ai/ha of 2,4-D and 0.82 kg ai/ha of dicamba. D1, D3, D7, D14, and D29 represent applying herbicides 14 hours, 3, 7, 14, and 29 days, respectively, after cotton stalks were shredded

Table 3 shows the means for the four vegetation indices among the eight herbicide treatments based on the CIR image. The means for visual rating are also shown in the table. The four vegetation indices detected two significantly different groups among the eight treatments. Regrowth from treatments 1 and 7 had higher values for the four vegetation indices than regrowth from the other six treatments. Thus, treatments 1 and 7 had more regrowth and were less effective than the other treatments. However, no statistical differences were detected between treatments 1 and 7, nor were significant differences found among treatments 2, 3, 4, 5, 6 and 8. These results generally agreed with those from the visual analysis of the spectra and the airborne CIR imagery.

Table 3 Comparisons of means for four vegetation indices and one visual rating index among eight herbicide treatments based on an airborne color-infrared image and ground rating data obtained 36 days after cotton stalks were shredded in a cotton field

Treatment ^[a]	NR ^[b]	NG	NDVI	GNDVI	Visual Rating ^[c]
1. Dicamba (D1) + 2,4-D (D29)	1.456a ^[d]	2.002a	0.185a	0.333a	3.00a
2. 2,4-D (D1) + 2,4-D (D29)	1.265b	1.737b	0.117b	0.269b	1.38c
3. Dicamba (D3) + 2,4-D (D29)	1.321b	1.807b	0.136b	0.285b	2.13b
4. 2,4-D (D3) + 2,4-D (D29)	1.267b	1.740b	0.117b	0.269b	1.50c
5. Dicamba (D7) + 2,4-D (D29)	1.289b	1.786b	0.126b	0.282b	2.00b
6. 2,4-D (D7) + 2,4-D (D29)	1.279b	1.774b	0.121b	0.278b	1.50c
7. Dicamba (D14) + 2,4-D (D29)	1.436a	1.983a	0.178a	0.329a	3.00a
8. 2,4-D (D14) + 2,4-D (D29)	1.271b	1.775b	0.119b	0.278b	1.50c

Note: ^[a] Application rates were 1.06 kg ai/ha of 2,4-D and 0.82 kg ai/ha of dicamba. D1, D3, D7, D14, and D29 represent applying herbicides 14 hours, 3, 7, 14, and 29 days, respectively, after cotton stalks were shredded.

^[b] NR = NIR/Red, NG = NIR/Green, NDVI = (NIR-Red)/(NIR+Red), and GNDVI = (NIR-Green)/(NIR+Green).

^[c] Rating scale: 1-no live plants; 2-some plants alive, but exhibit herbicide damage; 3-most plants alive, but exhibit herbicide damage; 4-some plants appear healthy; and 5-most plants appear healthy.

^[d] Means within a column followed by the same letter are not significantly different at the 0.05 level according to Fisher's protected LSD procedure following an analysis of variance on a randomized complete block design.

Three statistically distinct groups were identified among the eight treatments based on visual rating. As detected by the image data, treatments 1 and 7 had a significantly higher visual rating than the other six treatments. However, based on visual rating, the six

treatments were further separated into two groups with treatments 3 and 5 as one and treatments 2, 4, 6, and 8 as the other. Treatments 3 and 5 had slightly higher visual rating values than treatments 2, 4, 6, and 8. Although the image data did not separate treatments 3 and 5 from treatments 2, 4, 6 and 8 at the 0.05 probability level, the spectral values coincided with the ground visual rating values. In fact, the correlation coefficients between visual rating and each of the four spectral variables were 0.974 for NR, 0.967 for NG, 0.976 for NDVI, and 0.968 for GNDVI. Based on the results of the 2002 experiment, 2,4-D applied to shredded cotton stalks at 1.06 kg ai/ha twice within a one-month period provided excellent regrowth control, while dicamba applied at 0.82 kg ai/ha followed by a 2,4-D application was not as effective.

3.3 Cotton root rot

Figure 5 shows a CIR image and its two-zone classification map for the 105-ha center-pivot irrigated cotton field in the 2001 study. On the CIR image, healthy plants showed a reddish-magenta tone, while infected plants had a greenish or dark color. The root rot areas could be easily separated from the healthy areas on the CIR image. By the time the images were acquired, most of the infected plants were dead, with their brown leaves attached to the plants. Plants that succumbed to the fungus earlier in the season bore only a few bolls or no bolls at all, while plants that succumbed later in the season bore a significant number of bolls. On the classification map, the red color represents root rot-infested areas, while the green color depicts healthy areas. A visual comparison of the classification map and the CIR image revealed that the two-zone classification map effectively identified apparent root rot areas within the field. The percentage of root rot areas was 17.1% for the irrigated field.

Table 4 shows an accuracy assessment error matrix for the classification map of the irrigated field. The error matrix was generated by comparing the classified categories with the ground observations at the 50 sites within the field. The overall accuracy of the classification map was 98%, indicating that the probability of image pixels being correctly identified in

the classification map is 98%. In addition to the overall accuracy, the producer's accuracy and the user's accuracy are commonly used for accuracy assessment. The producer's accuracy (a measure of omission error), which indicates the probability of actual areas being correctly classified, was 100% for the root rot category and 96.8% for the healthy category. This omission error was due to the small inclusions of healthy plants within large root rot areas. The user's accuracy (a measure of commission error), which is indicative of the probability that a category classified on the map actually represents that category on the ground, was 95% for the root rot areas and 100% for the healthy areas. Another accuracy measure, the kappa estimate for this field, was 0.958, indicating that the classification achieved an accuracy that is 95.8% better than would be expected from random assignment of pixels to categories.

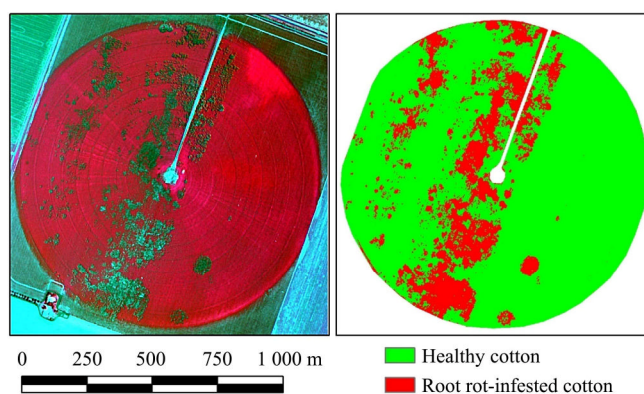


Figure 5 Color-infrared image and its corresponding classification map for a 105-ha irrigated cotton field infected with root rot in south Texas

Table 4 Error matrix for a two-zone classification map of a color-infrared image for a 105 ha irrigated field infected with cotton root rot

Classified Category	Actual Category		Total	User's Accuracy
	Root Rot	Healthy		
Root rot	19	1	20	95.0%
Healthy	0	30	30	100.0%
Total	19	31	50	
Producer's accuracy	100.0%	96.8%		

Note: Overall accuracy = (19 + 30)/50 = 98.0%. Kappa = 0.958.

It should be noted that root rot was the dominant stress in the study field, even though other minor stresses may have been present. Some pest insects such as boll weevils may have caused the reduction in yield, but they

had little effect on the plant canopy. Therefore, this type of infestation did not affect the correct identification of root rot areas within the field. Stresses that could cause plant wilting or death, as root rot did, would significantly affect the accuracy of the root rot mapping results. However, based on the limited number of sites verified on the ground, all classified root rot sites actually had root rot and no other stresses were identified.

Image classifications of the multispectral and hyperspectral images acquired from the 55-ha center-pivot irrigated field in 2002 showed that root rot-infected areas were 30.7% from the multispectral image and 30.5% from the hyperspectral image for the field. Accuracy assessment of the classification maps showed that both types of images provided the same overall accuracy of 98%. These results clearly indicate that both airborne multispectral and hyperspectral imagery can be successfully used for assessing root rot damage within cotton fields.

Table 5 summarizes plant density, boll density, seed cotton yield, and lint yield for root rot and healthy areas for the 105-ha field. Plant density was statistically the same in the root rot and healthy areas within the field. However, boll density was 31.6 bolls/m² or 42% lower in the root rot areas than in the healthy areas. Both seed cotton yield and lint yield were approximately 47% lower in the root rot areas for the field. Root rot decreased lint yield by 732 kg/ha.

Table 5 Means of plant density, boll density, seed cotton yield, and lint yield between root rot and healthy zones within a 105 ha irrigated field

Classification zone	Plant density /plants·m ⁻²	Boll density /bolls·m ⁻²	Seed cotton yield/kg·ha ⁻¹	Lint yield /kg·ha ⁻¹
Root Rot	13.8a ^[a]	44.3b	2055b	831b
Healthy	13.6a	75.9a	3930a	1563a

Note: ^[a] Means within a column followed by the same letter are not significantly different at the 0.05 level.

Table 6 summarizes cotton fiber properties for root rot and healthy areas for the 105-ha field. Micronaire is the standard estimate of both fineness and maturity in the USDA Agricultural Marketing Service classing offices. The acceptable upland micronaire range for which no price penalty is assessed is 3.5 to 4.9, with a premium range of 3.7 to 4.2^[24]. The micronaire reading for the

root rot cotton fell below the premium range, while the reading for the healthy cotton was just within the premium range. Upper half mean length (UHM) measures the average length of the longer half of the fibers. No significant difference in UHM was found between root rot and healthy cotton for the irrigated field. Length uniform index (UI) was slightly higher for healthy cotton than for root rot cotton. Healthy cotton had higher fiber strength than root rot cotton. The degree of reflectance (Rd) and yellowness (+b) are used as a measure of the color of cotton. No significant differences in Rd and +b were found between root rot and healthy cotton for the field.

Table 6 Means of cotton fiber properties between root rot and healthy zones within a 105 ha irrigated field

Classification Zone	Micro-naire	UHM /mm	UI /%	Strength /g·tex ⁻¹	Rd /%	+b
Root rot	2.7b ^[a]	30a	83.3b	30.6b	77.2a	7.4a
Healthy	3.9a	30a	84.8a	33.3a	78.3a	7.7a

Note: ^[a] Means within a column followed by the same letter are not significantly different at the 0.05 level.

One important step toward the management of cotton root rot is to accurately delineate infected areas within a field. Unsupervised classification maps created from airborne multispectral imagery can effectively identify root rot areas. However, one problem associated with the direct use of the classification map for management is that the infected areas may expand over the following season. In order to account for the possible expansion of the fungus in the production of root rot treatment maps, buffer zones around the root rot areas need to be created. For example, if a buffer distance of 1 m is used to create a buffer zone on the infected areas for the 105-ha cotton field, the percentage of root rot treatment areas over the total area would increase from 17.1% to 22.5% based on image analysis. For buffer distances of 2 to 10 m, the percentage treatment area will vary from 26.7% to 47.7%. The selection of buffer distances can be based on the expansion speed of the fungus. If the spread of the fungus is minimal and slow, maps with smaller buffer distances should be used. Otherwise, maps with larger buffer distances are necessary to ensure that more areas than the infected areas are included. Too small a buffer

could mean an infected area may be missed, leading to yield loss and faster reinfection of the field. On the other hand, too large a buffer may create some waste and economic loss. Any treatment that costs more than the gain in gross revenue may not be feasible since this fungus can hardly be eliminated and has to be treated every year or every few years to suppress it.

4 Conclusions

Results from these studies demonstrate that remote sensing can be a useful tool for evaluating the effectiveness of cotton defoliation and regrowth control strategies and for mapping root rot damage in cotton fields. Compared with traditional visual observations and ground measurements, remote sensing techniques have the potential for more effective and accurate assessments of various cotton production operations and pest conditions.

Ground reflectance spectra offer spectral observations over continuous wavelengths at selected sites from each treatment and can be used to differentiate among chemical treatments for cotton defoliation and regrowth control. However, a sufficient number of spectra are needed from each treatment to accommodate the within-treatment variability. Thus this approach can be time-consuming. On the other hand, airborne digital imagery provides a continuous view of all treatment plots and has the potential for quick visual comparisons among the treatments. Moreover, airborne imagery contains spectral information for every area of the field and allows quantitative separations of the treatments using the spectral bands and vegetation indices derived from these bands. Airborne digital imagery is more effective and reliable than reflectance spectra for this type of applications. Compared with traditional methods, the airborne imagery-based approach is more efficient and effective if a large number of treatments are to be evaluated over large areas. Certainly, limited ground measurements and observations are necessary to validate the remote sensing results.

Airborne multispectral and hyperspectral imagery in conjunction with image classification techniques can be very effective for detecting and mapping cotton root rot.

Both types of imagery can equally accurately distinguish root rot-infected areas from non-infected areas. Therefore, multispectral imagery is more appropriate for mapping root rot infection because it is cheaper and more widely available than hyperspectral imagery. Classification maps with buffer zones covering root rot areas and the potential spread of the disease can be used for site-specific management of the recurring root rot disease in the following seasons. However, if there exist multiple stresses with similar symptoms to root rot within the field, high spatial resolution multispectral and/or hyperspectral imagery taken at multiple times may be necessary along with the knowledge of the dynamic processes of the co-occurring stresses. As remote sensing imagery is becoming more available and less expensive, it will present a great opportunity for both cotton growers and researchers to use this type of data for cotton production and pest management.

Acknowledgements

The authors thank Rene Davis and Fred Gomez of USDA-ARS, Weslaco, Texas for image acquisition and Jim Forward of USDA-ARS, Weslaco, Texas for assistance in ground reflectance measurements and image processing. Thanks are also extended to Bill Harper of Texas A&M at Corpus Christi, Texas for ground data collection and Randy Rachel of Corpus Christi, Texas for the use of his field for the root rot study.

[References]

- [1] Cothren J T, Witten T K. How do harvest aids work? In Proc. Beltwide Cotton Production Conferences, 69. Memphis, Tennessee: National Cotton Council of America. 2001
- [2] Keeling W. Southwest cotton harvest aid performance and narrow row options. In Proc. Beltwide Cotton Production Conferences, 72. Memphis, Tennessee: National Cotton Council of America. 2001.
- [3] Warrick B E. Evaluation of Action as a cotton harvest aid in west central Texas. In Proc. Beltwide Cotton Production Conferences, 507-511. Memphis, Tennessee: National Cotton Council of America. 2001.
- [4] Norman J W Jr., Greenberg S M, Sparks A N Jr., Stichler C. Termination of cotton stalks with herbicides in the Lower Rio Grande Valley of Texas. In Proc. Beltwide Cotton Production Conferences. Memphis, Tennessee: National Cotton Council

- of America. 2003. CDROM.
- [5] Sparks A N Jr, Norman J W Jr, Stichler C, Bremer J, Greenberg S. Cotton stalk destruction with selected herbicides and effects of application methodology. In Proc. Beltwide Cotton Production Conferences. Memphis, Tennessee: National Cotton Council of America. 2002. CDROM.
- [6] Yang C, Greenberg S M, Everitt J H, Sappington T W, Norman J W Jr. Evaluation of cotton defoliation strategies using airborne multispectral imagery. Transactions of the ASAE, 2003; 46(3): 869-876.
- [7] Yang C, Greenberg S M, Everitt J H. Evaluation of herbicide-based cotton regrowth control using remote sensing. Transactions of the ASAE, 2005; 48(5): 1987-1994.
- [8] Yang C, Greenberg S M, Everitt J H, Norman J W Jr. Assessing cotton stalk destruction with herbicides using remote sensing technology. Journal of Cotton Science, 2006; 10(2): 136-145.
- [9] Smith H E, Elliot F C, Bird L S. Root rot losses of cotton can be reduced. Pub. No. MP361. The Texas A&M University System, Texas Agricultural Extension Service, College Station, Texas. 1962.
- [10] Ezekiel W N, Taubehaus J J. Cotton crop losses from phymatotrichum root rot. J. Agric. Res., 1934; 49(9): 843-858.
- [11] Taubehaus J J, Ezekiel W N. The quality of lint and seed from cotton plants with phymatotrichum root rot. Phytopathology, 1935; 25: 104-113.
- [12] Lyda S D, Robison G D, Lembright H W. Soil fumigation control of phymatotrichum root rot in Nevada. Plant Disease Reporter, 1967; 51(5): 331-333.
- [13] Rush C M, Lyda S D. Effects of anhydrous ammonia on mycelium and sclerotia of *Phymatotrichum omnivorum*. Phytopathology, 1982; 72: 1085-1089.
- [14] Rush C M, Gerik T J. Relationship between postharvest management of grain sorghum and *Phymatotrichum* root rot in the subsequent cotton crop. Plant Disease, 1989; 73(4): 304-305.
- [15] Taubehaus J J, Ezekiel W N, Neblette C B. Airplane photography in the study of cotton root rot. Phytopathology, 1929; 19: 1025-1029.
- [16] Nixon P R, Lyda S D, Heilman M D, Bowen R L. Incidence and control of cotton root rot observed with color infrared photography. Pub. No. MP1241. The Texas A&M University System, Texas Agricultural Experiment Station, College Station, Texas. 1975.
- [17] Nixon P R, Escobar D E, Bowen R L. A multispectral false-color video imaging system for remote sensing applications. In Proc. 11th Biennial Workshop on Color Aerial Photography and Videography in the Plant Sciences and Related Fields, 295-305, 340. Bethesda, Maryland: American Society for Photogrammetry and Remote Sensing. 1987.
- [18] Yang C, Fernandez C J, Everitt J H. Mapping *Phymatotrichum* root rot of cotton using airborne three-band digital imagery. Transactions of the ASAE, 2005; 48(4): 1619-1626.
- [19] Yang C, Fernandez C J, Everitt J H. Comparison of airborne multispectral and hyperspectral imagery for mapping cotton root rot. Biosystems Engineering, 2010; 107: 131-139. 2010.
- [20] Escobar D E, Everitt J H, Noriega J R, Davis M R, Cavazos I. A true digital imaging system for remote sensing applications. In Proc. 16th Biennial Workshop on Color Photography and Videography in Resource Assessment, 470-484. Bethesda, Maryland: American Society for Photogrammetry and Remote Sensing. 1997.
- [21] Yang C, Everitt J H, Davis M R, Mao C. A CCD camera-based hyperspectral imaging system for stationary and airborne applications. Geocarto International Journal, 2003; 18(2): 71-80.
- [22] Yang C, Everitt J H. Relationships between yield monitor data and airborne multispectral multirate digital imagery for grain sorghum. Precision Agriculture, 2002; 3(4): 373-388.
- [23] Schowengerdt R A. Remote sensing models and methods for image processing, 2nd ed. San Diego, California: Academic Press. 1997.
- [24] Bradow J M, Davidonis G H. Quantitation of fiber quality and the cotton production processing interface: A physiologist's perspective. J. Cotton Sci., 2000; 4(1): 34-64.
- [25] Campbell J B. Introduction to remote sensing, 3rd ed. New York: The Guilford Press. 2002.